



Storage of very cold neutrons in a trap with nano-structured walls

E.V. Lychagin^c, A.Yu. Muzychka^c, V.V. Nesvizhevsky^{a,*}, G. Pignol^b, K.V. Protasov^b, A.V. Strelkov^c

^a ILL, 6 rue Jules Horowitz, Grenoble F-38042, France

^b LPSC (UJF, CRNS/IN2P3, INPG), 53, rue des Martyrs, Grenoble F-38026, France

^c JINR, 6 Joliot-Curie, Dubna, Moscow reg. 141980, Russia

ARTICLE INFO

Article history:

Received 9 December 2008

Received in revised form 27 March 2009

Accepted 15 July 2009

Available online 21 July 2009

Editor: V. Metag

Keywords:

Very cold neutrons

Diamond nanoparticles

Neutron scattering

Fundamental particle physics

ABSTRACT

We report on storage of Very Cold Neutrons (VCN) in a trap with walls containing powder of diamond nanoparticles. The efficient VCN reflection is provided by multiple diffusive elastic scattering of VCN at single nanoparticles in powder. The VCN storage times are sufficiently long for accumulating large density of neutrons with complete VCN energy range of up to a few times 10^{-4} eV. Methods for further improvements of VCN storage times are discussed.

© 2009 Elsevier B.V. All rights reserved.

1. Introduction

Recently we showed that powders of nanoparticles could be used efficiently as first reflectors for Very Cold Neutrons (VCN) in the velocity range of up to 160 m/s [1], thus bridging the energy gap between efficient reactor reflectors [2] for thermal and cold neutrons, and optical neutron-matter potential for ultracold neutrons (UCN) [3].

The use of nanoparticles provides a sufficiently large cross-section for coherent scattering and inhomogeneity of the moderator/reflector density on a spatial scale of about the neutron wavelength [4]. A large number of diffusive collisions needed to reflect VCN from powder constrains the choice of materials: only low-absorbing ones with high optical potential are appropriate. Thus, diamond nanoparticles were an evident candidate for such VCN reflector. The formation of diamond nanoparticles by explosive shock was first observed more than forty years ago [5]. Since then very intensive studies of their production and of their various applications have been performed worldwide. These particles measure a few nanometers; they consist of a diamond nucleus (with a typical diamond density and optical potential) within an onion-like shell with a complex chemical composition [6] (with lower optical potential). A recent review of the synthesis, structure, properties and applications of diamond nanoparticles can be found in [7].

The first experiments on the reflection of VCN from nano-structured materials as well as on VCN storage were carried out in the seventies [8] and later continued in Ref. [9]. In [1] we extended significantly the energy range and the efficiency of VCN reflection by exploiting diamond nanoparticles. A reflector of this type is particularly useful for both UCN sources using ultracold nanoparticles [4,10] and for VCN sources; it would not be efficient however for cold and thermal neutrons, as shown in [11].

In order to measure precisely the VCN reflection probability from powder of diamond nanoparticles and to explore feasibility of VCN storage in traps with nano-structured walls, we carry out a dedicated experiment described in the present Letter. In fact, the measuring procedure used here is equivalent to that typically used in experiments on UCN storage in traps (see for example [12,13]). The difference consists in a type of trap walls and in characteristic values of the reflection probability. In Section 2 we describe the experimental setup. In Section 3 we present the experimental results, and analyze them in Section 4.

2. The experimental setup

This experiment was carried out at the VCN beam, PF2, ILL. The installation scheme is shown in Fig. 1.

The VCN trap has cylindrical shape with a diameter of 44 cm and a height of 47 cm. VCN could enter the trap through a small square window of 2 cm by 2 cm in its side wall. The VCN beam diameter is ≈ 1 cm. VCN could be reflected many times from the trap walls. Thus they could find an exit circular window with a diameter of 6 cm in the trap cover and enter into a detector behind

* Corresponding author.

E-mail address: nesvizhevsky@ill.fr (V.V. Nesvizhevsky).

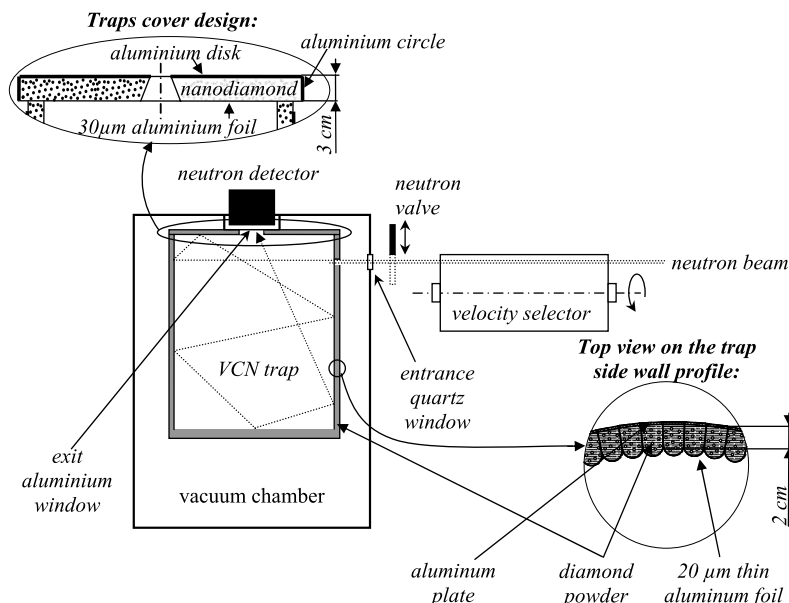


Fig. 1. The installation scheme.

the window. The VCN beam could be opened or closed using a fast cadmium valve with a thickness of 0.2 mm. The VCN velocity could be chosen using a velocity selector in front of the valve. The trap is placed inside a vacuum chamber with an entrance quartz window with a thickness of 3 mm and an exit aluminum window with a thickness of 1 mm. When the VCN beam is closed the detector count rate decreases exponentially following the VCN density in the trap. Thus we could measure the VCN storage times as a function of their velocity.

The neutron detector is a gaseous proportional ^3He counter (the thickness of its sensitive layer is 5 cm, the ^3He partial pressure is 200 mbar) with an entrance aluminum window with a thickness of 100 μm and a diameter of 9 cm. The electrical detector signals are analyzed using time and amplitude information.

The velocity selector consists of a cylinder with a length of $l = 40$ cm and a diameter of $D = 19$ cm. Curved plastic plates with a thickness of 1 mm are installed at the side surface of the cylinder in such a way that they form screw-like slits with a width of $d \approx 4.5$ mm and the screw length of $L = 480$ cm. The cylinder rotates around its axis with the period T . Neutrons could scatter at hydrogen atoms in the plate's material; those neutrons leave the neutron beam. The rotation period defines the velocity of neutrons passing through the selector. Neutrons with low angular divergence and with momentum parallel to the selector axis pass through the selector screw slits, thus avoiding scattering by the plates only if the neutron velocity is equal to

$$v = L \frac{2\pi}{T} \left(1 \pm \frac{dL}{2\pi D l} \right). \quad (1)$$

The selector allowed us to choose the neutrons with a velocity in the range of 30–160 m/s. The velocity resolution was measured using time-of-flight method; the result is shown in Fig. 2. It is equal to 10% if $v = 160$ m/s, and 25% if $v = 30$ m/s. The neutron flux at the selector exit is shown in Fig. 3.

The valve is controlled by an electro-magnet governed with an electric pulse generator. The time of opening and closing the valve was measured in a separate experiment with a light beam; it is equal to 5 ms in both cases.

The trap is built using powder of diamond nanoparticles. In order to build the trap side walls we filled the powder in aluminum

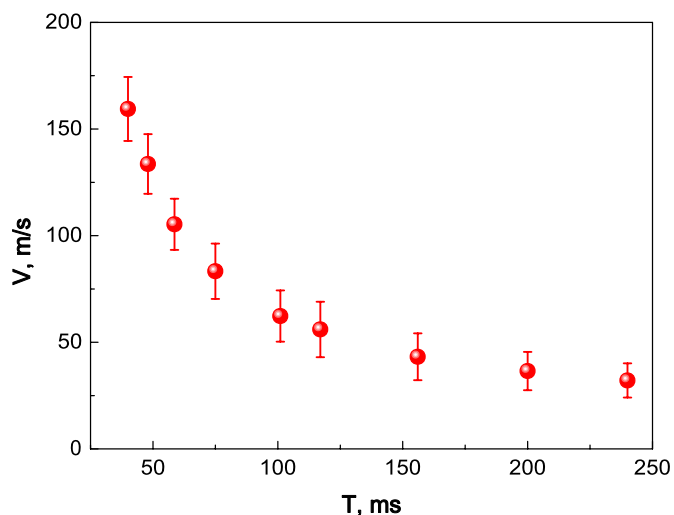


Fig. 2. The neutron velocity at the velocity selector exit is shown as a function of its rotation period. Error bars indicate the half width of velocity distribution in the beam after selector (these distributions are not Gaussians).

tubes and compressed it to the density of 0.4 g/cm^3 , then assembled the tubes into a cylinder, as shown in Fig. 1 and in Fig. 4; thus the side walls are not quite homogeneous. VCN reflect many times from powder; thus they pass many times through the aluminum walls of the tubes. In order to avoid significant losses of VCN in aluminum, we decreased the aluminum wall thickness to 20 μm . The trap cover is shown in Fig. 1 and in Fig. 5. It consists of an aluminum disk, an aluminum circle fixed to its perimeter; a foil with a thickness of 30 μm attached as shown in Fig. 1 and in Fig. 5, and a 3 cm thick powder layer over the aluminum foil. The powder density in the trap cover is 0.3 g/cm^3 . A hole in the cover center (see Figs. 1 and 5) allows us to count VCN in the detector. The cover is installed on top of the trap side wall thus an eventual slit between the side wall and the cover is minimized. The trap bottom is covered with powder with a thickness of 3 cm compressed to a density of 0.3 g/cm^3 .

Electro-heaters are rolled around the trap; the trap and the electro-heaters are covered by many aluminum foil layers in or-

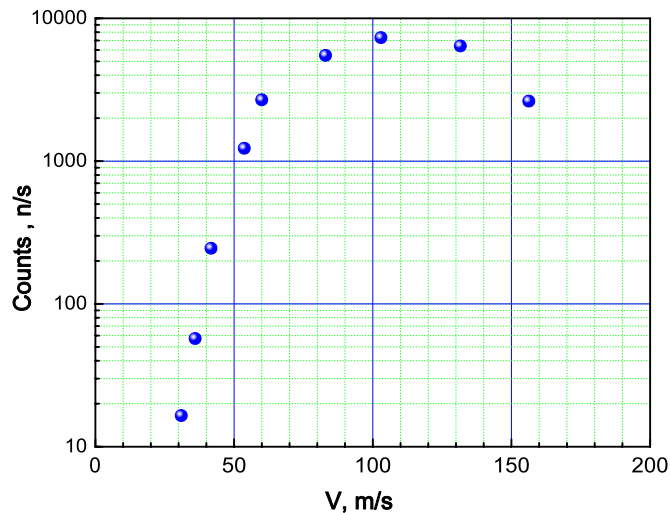


Fig. 3. The neutron flux at the selector exit is shown as a function of the neutron velocity.



Fig. 4. The VCN trap. The cover is open.



Fig. 5. The cover with a window in its center.

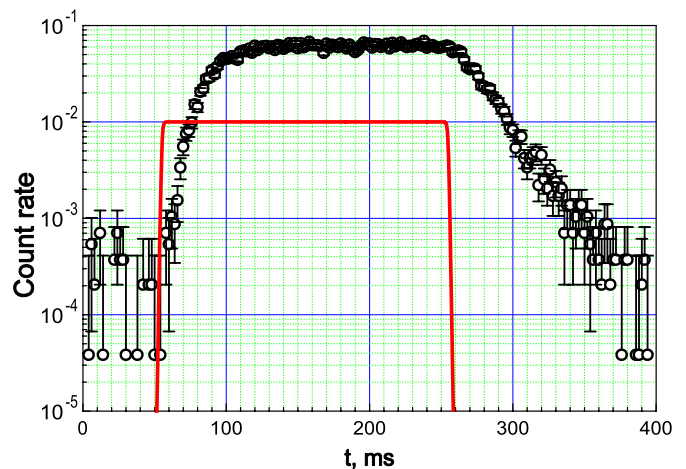


Fig. 6. An example of the neutron count rate during a measurement cycle for the VCN velocity of 85 m/s. The solid line shows the light signal, in arbitrary units, used to synchronize the valve with the measurement cycle.

der to provide thermal isolation of the trap. The trap temperature could be raised using the electro-heaters and measured with two thermo-pairs attached to the massive aluminum parts of the trap bottom and the cover respectively.

3. The experimental results

When the valve is open VCN fill in the trap as long as needed to reach a saturation VCN density. Then we close the valve and measure the time constant of the exponential decrease of the VCN density in the trap. The detector count rate is proportional to the VCN density in the trap. Such a measuring cycle is repeated many times in order to accumulate sufficient statistics.

An example of the neutron count rate during one cycle is shown in Fig. 6; a background is subtracted. The solid line in Fig. 6 shows the light signal, in arbitrary units, used to synchronize the valve with the measuring cycle. A pulse generator starts the cycle at time $t = 0$, opens the valve at $t = 50$ ms, and closes the valve at $t = 250$ ms. When the valve is open the trap could be filled in with VCN up to a saturation density. When the valve is closed, the VCN density decreases exponentially. The characteristic time of this decrease is equal to a convolution of the VCN storage time and emptying time. The dominant loss factor is associated with the trap walls, as the area of the entrance and exit windows is smaller than 0.3% compared to total area of the trap surface. The storage time in Fig. 6 is equal to $\tau_{st}^{VCN} = (19.0 \pm 0.5)$ ms.

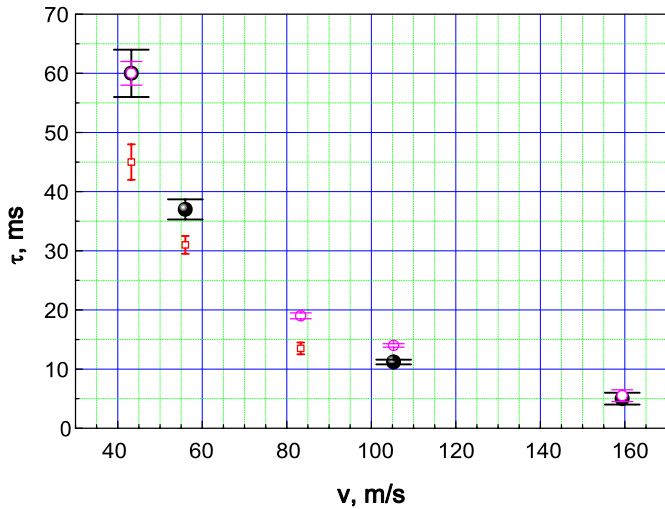


Fig. 7. The VCN storage times as a function of their velocity. Black circles correspond to measurements at ambient temperature after 12 hour pumping. Empty circles show measurements at ambient temperature after heating the trap at 120 °C in argon. Boxes indicate results obtained at a temperature of 150 °C under permanent pumping.

Analogous measurements were carried out for this and other VCN velocities in 3 series of measurements. First, we pumped out the trap during 12 hours then measured the VCN storage times at ambient temperature. Second, the vacuum chamber was filled in with argon at a pressure of 1 bar then the trap was heated to a temperature of ≈ 120 °C and kept at this temperature during 3 hours. After that argon was pumped out, the trap was slowly cooled to ambient temperature then VCN storage times were measured. Third, we heated the trap to a temperature of ≈ 145 °C on permanent pumping. The measurement started when the temperature (measured with the two thermo-pairs) had got stabilized. Besides, the detector count rate had to get stabilized as well in the configuration with the valve open and the neutron velocity equal to 160 m/s; the largest velocity corresponds to the highest sensitivity to VCN losses. The detector count rate stabilization is delayed because of slow heating of internal zones of powder.

The results of all these 3 series of measurements are shown in Fig. 7. Storage times were not measured for fast neutrons in the third series, because they are too short.

As clear from Fig. 7, the trap degassing does not increase the neutron storage times as compared with those for the pumped trap; though increase of the trap temperature to 150 °C (30% in absolute scale) decreases neutron storage times by 30%. It looks like increasing the neutron losses due to inelastic scattering by hydrogen bounded strongly to the diamond (it is not removed by 150 °C degassing).

4. Analysis of the experimental results

For the trap geometry described above we calculate a VCN mean free path for all neutron velocities equal:

$$\Delta x = 22 \pm 1 \text{ cm}, \quad (2)$$

neglecting small gravitational corrections. Thus the probability of VCN reflection from the trap wall is equal to:

$$P(v) = 1 - \frac{v}{\tau_{st}^{VCN} \Delta x} (1 - \epsilon) \quad (3)$$

where ϵ is a geometrical factor equal to the ratio of the probability of losses in the entrance and exit windows to the total probability

of losses in the trap. $\epsilon = 3.5 \times 10^{-3}$. The error bars in this estimation are defined by uncertainties of the storage time (see Fig. 7), the mean flight pass and the neutron velocity (see Fig. 2).

This probability represents the reflectivity for the walls actually used in this experiment. It thus includes losses in the aluminium foil, and effects of the geometrical shape of the trap walls. This estimation supposes isotropic angle distribution of neutrons in the trap that is not quite true for fast neutrons.

On the other hand, we have in hand a model for the propagation of neutrons in the nanoparticle powder. The method used here to describe the reflection of VCN at a layer of nanoparticles is similar to that in [1]. Namely, we neglected the relatively complex internal structure of the nanoparticle and modeled it as a uniform sphere, which is possible as the neutron wavelength is large as compared to the nanoparticle size. The neutron-nanoparticle elementary interaction was calculated using the first Born approximation. The amplitude for a neutron with the energy $(\hbar k)^2/(2m)$ to be scattered at a spherical nanoparticle with the radius R and the optical potential V , at an angle θ is equal:

$$f(\theta) = -\frac{2m}{\hbar^2} V R^3 \left(\frac{\sin(qR)}{(qR)^3} - \frac{\cos(qR)}{(qR)^2} \right) \quad (4)$$

where $q = 2k \sin(\theta)$ is the transferred momentum. The total elastic cross section is written correspondingly:

$$\sigma_s = \int |f|^2 d\Omega = 2\pi \left| \frac{2m}{\hbar^2} V \right|^2 R^6 \frac{1}{(kR)^2} I(kR), \quad (5)$$

where

$$I(kR) = \frac{1}{4} \left(1 - \frac{1}{(2kR)^2} + \frac{\sin(4kR)}{(2kR)^3} - \frac{\sin^2(2kR)}{(2kR)^4} \right). \quad (6)$$

The chemical composition of the nanoparticle is complex and includes carbon (up to 88% of the total mass), hydrogen (1%), nitrogen (2.5%), oxygen (up to 10%) [14]. Moreover, a certain amount of water covers a significant surface area of the nanoparticles. In general, the hydrogen in the water and on the surface of the nanoparticles scatters the neutrons up to the thermal energy range (*up-scattering*); thermal neutrons do not interact as efficiently with nanoparticles and therefore traverse powder. The hydrogen quantity in the powder was measured by (n, γ) method. The composition $C_{15}H$ was found for degassed and non degassed powder in vacuum; composition C_8H was found for powder in air.

To compare the experimental results to the model of independent nanoparticles, we further corrected the measured reflectivity for VCN losses in the aluminum foils as well as for a dead zone in the wall structure between neighbor cylinders. The corrected reflectivity is shown in Fig. 8 for measurements at ambient temperature (averaged over two series of measurements) together with the Monte Carlo calculation. The only free parameter of this calculation concerns inelastic scattering on hydrogen. In the Monte Carlo simulation, the quantity of hydrogen is fixed according to the $C_{15}H$ chemical composition (0.5% of the total mass). Besides, the cross section for inelastic scattering is assumed to follow the $1/v$ rule, and the value of the cross section σ_H for the neutron velocity of 2200 m/s is considered as an effective parameter. The calculation reproduces well the velocity dependence of the reflectivity; the effective parameter is fitted with the approximate value of $\sigma_H = 1.3$ barn.

5. Conclusion

We have observed for the first time the storage of VCN with velocities in the range of 40–160 m/s (the energy up to 10^{-4} eV) in a trap with walls composed of powder of diamond nanoparticles.

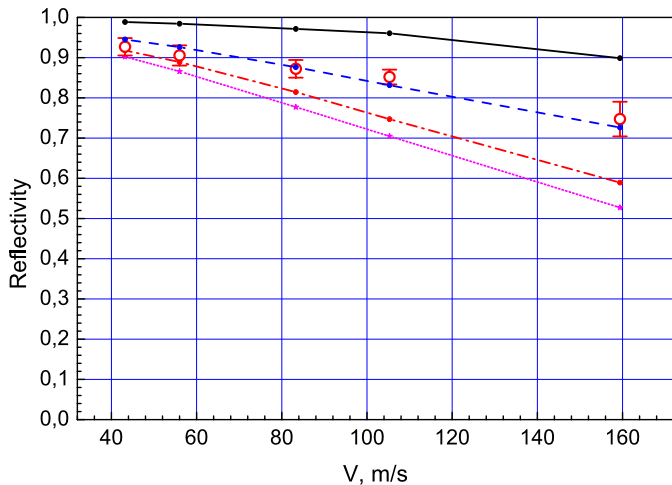


Fig. 8. The probability of VCN reflection from a layer of nanoparticles at ambient temperature is shown with empty circles as a function of their velocity. Thin lines correspond to Monte Carlo calculations taking into account up-scattering at hydrogen, the quoted cross section corresponds to the neutron velocity of 2200 m/s: 4 barn for dotted pink line, 3 barn for dot-dashed red line, 1.3 barn for dashed blue line and 0 barn for plain black line.

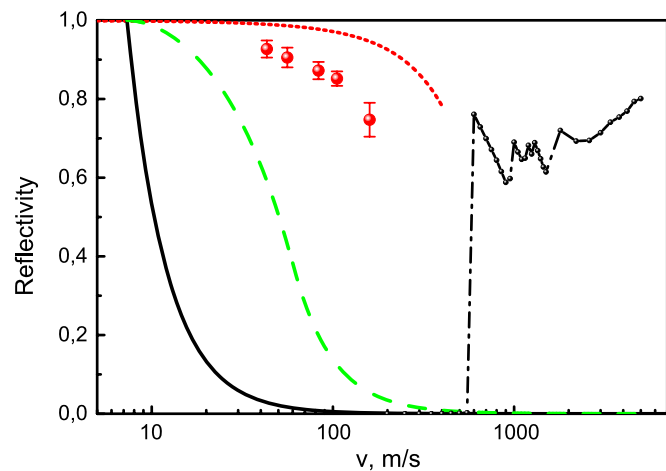


Fig. 9. The elastic reflection probability for isotropic neutron flux is shown as a function of the neutron velocity for various carbon-based reflectors: (1) Diamond-like coating (DLC) (thin solid line), (2) The best supermirror [16] (dashed line), (3) Hydrogen-free ultradiamond [15] powder with the infinite thickness (dotted line). Calculation. (4) VCN reflection from 3 cm thick diamond nanopowder at ambient temperature (points), with significant hydrogen contamination [this Letter]. Experiment. (5) MCNP calculation for reactor graphite reflector [2] with the infinite thickness at ambient temperature.

The VCN storage will allow us to accumulate significant number (density) of VCN in a trap (much larger than that typical for UCN). Such a trap can be used as a reflector for VCN sources and in some cases for UCN sources. Further improvement of the VCN storage times could be achieved by removing a part of hydrogen from powder and by cooling the trap to a temperature, at which the inelastic up-scattering of VCN at hydrogen is suppressed. Another option could consist in replacing the diamond nanoparticles by O_2 , D_2 , D_2O , CO_2 , CO or other low-absorbing nanoparticles, free of hydrogen and other impurities with significant VCN loss cross-section.

The probability of cold neutron isotropic flux reflection from diamond nanoparticles is compared with others well known reflectors in Fig. 9. As clear from Fig. 9, the maximum energy of the reflected VCN and the reflection probability far exceeds the corresponding values for the best supermirrors available [16]. Thus nanoparticle reflector bridges the energy gap between efficient reactor reflectors for thermal and cold neutrons, and the optical potential for UCN. This phenomenon has a number of applications. Such a reflector can be used for VCN and UCN sources, for more efficient guiding of VCN and, probably, of even faster neutrons at quasi-specular trajectories.

References

- [1] V.V. Nesvizhevsky, et al., Nucl. Instrum. Methods A 595 (2008) 631.
- [2] E. Fermi, A course in neutron physics, in: Collected Papers, The University of Chicago Press, Chicago, 1965.
- [3] V.I. Luschikov, Yu.N. Pokotilovsky, A.V. Strelkov, F.L. Shapiro, JETP Lett. 9 (1) (1969) 23.
- [4] V.V. Nesvizhevsky, Phys. At. Nucl. 65 (2002) 400.
- [5] P.J. De Carli, J.C. Jamieson, Science 133 (1961) 1821.
- [6] A.E. Aleksenskii, M.V. Baidakova, A.Y. Vul', V.I. Siklitskii, Phys. Solid State 41 (1999) 668.
- [7] V.Yu. Dolmatov, Russ. Chem. Rev. 76 (2007) 339.
- [8] A. Steyerl, W.-D. Trüstedt, Z. Phys. 267 (1974) 379.
- [9] S.S. Arzumanov, et al., Phys. At. Nucl. 68 (2005) 1141.
- [10] V.V. Nesvizhevsky, G. Pignol, K.V. Protasov, Int. J. Nanosci. 6 (6) (2007) 485.
- [11] V.A. Artem'ev, At. Energy 101 (2006) 901.
- [12] V.K. Ignatovich, The Physics of Ultracold Neutrons, Oxford University Press, 1990.
- [13] R. Golub, D. Richardson, S.K. Lamoreaux, Ultra-Cold Neutrons, Adam Higler, 1991.
- [14] A.L. Vereschagin, G.V. Sakovich, V.F. Komarov, E.A. Petrov, Diamond Related Mater. 3 (1993) 160.
- [15] <http://www.ultradiamondtech.com>.
- [16] R. Maruyama, et al., Thin Solid Films 515 (2007) 5704.